Materials Research Express

ACCEPTED MANUSCRIPT

Modeling flow behavior of sintered Al–4%B₄C composite during high–temperature upsetting

To cite this article before publication: Seetharam R *et al* 2019 *Mater. Res. Express* in press https://doi.org/10.1088/2053-1591/ab6371

Modeling Flow Behavior of Sintered Al–4%B_4C Composite During High–Temperature Upsetting

[a]R. Seetharam, [b]S.K. Kanmani Subbu and [c]M.J. Davidson

[a]Department of Mechanical Engineering, Indian Institute of Information Technology, Design and Manufacturing, Kurnool 518007, Andhrapradesh, India.

[b]Department of Mechanical Engineering, Indian Institute of Technology, Palakkad 678557, Kerala, India.

[c]Department of Mechanical Engineering, National Institute of Technology, Warangal 506004, Telangana, India.

E-mail address: [a]seetharam.seetharam@gmail.com, [b]sksubbu@iitpkd.ac.in [c]mjdavidson2001@yahoo.co.in.

Abstract

The hot deformation behavior of sintered Al–4%B_4C composites was studied in this work. The main aim of this work is to estimate the effect of initial relative density (IRD), deformation temperature and strain rate on the hot deformation behavior and development of constitutive equations for predicting the hot deformation behavior. For this purpose, upsetting was performed in a hydraulic press for obtaining true stress–true strain curve data of sintered Al–4%B_4C composites. The tests were carried out at different IRDes of 80%, 85% and 90% for various temperatures of 573 K, 673 K and 773 K and strain rates of 0.1 s^{-1}, 0.2 s^{-1} and 0.3 s^{-1}. The test reveals that the effect of IRD, deformation temperature and strain rate on flow stress curves is significant. The constitutive equations have been developed for predicting the flow stress behavior during the hot upsetting of sintered Al–4%B_4C composite and it's validated with experiments. In addition, the required activation energies (Q) of sintered Al–4%B_4C composites during the hot upsetting were calculated for various IRDes of 80%, 85%, and 90% was 161.06, 172.28 and181.05 KJ/mol, respectively, which is higher than the value of pure aluminum (144.3 KJ/mol).

Keywords: Al–4%B_4C composite, Flow stress, Constitutive modeling, Hot upsetting, Activation energy.

1. Introduction

The metal matrix composite (MMC) materials have been used in several engineering applications successfully due to their attractive properties for the past four decades. MMCs properties such as specific stiffness, strength, creep resistance and wear resistance can be enhanced by adding selected reinforcement materials. In general, MMCs are fabricated by powder metallurgy (P/M) technique, which is demonstrated to be effective in reducing the defects and limitations of casting routes and also produce material with good quality properties. P/M technique is more being used in several engineering applications at large scale because of its less material utilization, less cost, less time, energy efficient operation and ease of automation. Cambronero et al. [1] reported that the physical and mechanical properties of AA7075 aluminium alloy with ceramic particle reinforcement were enhanced more, which are manufactured by the powder metallurgy process, for automobile applications. Nair et al. [2] stated that Al and its alloys reinforced with ceramic particles, which results in increased strength and reduced weight for the structural applications. Abenojar et al. [3] described the suitability of boron for nuclear applications due to its neutron absorption property. Boron carbide is one the hardest and lighter (density = 2.51 g/cc) material than other commercial reinforcement. B_4C is widely used as cermets and armor materials due to good wear resistance properties. William and Harrigan [4] studied the mechanical and thermal properties of aluminium matrix reinforced with B_4C particles. It is observed that the mechanical and thermal properties are enhanced by incorporating B_4C particles in aluminium matrix and the product cost is reduced when it is prepared by vacuum–hot pressing. There is increasing interest in Al–B_4C composites due to high hardness and strength to weight ratio. An Al–B_4C composite is used in defense, electronic and nuclear industries.

In the past few years, researchers are concentrating on the flow behavior of aluminium and its alloys for understanding the mechanical working processes. The knowledge about the hot deformation performance of the material is essential for optimizing the process parameters to get the desired products with excellent properties in the forming process. The flow stress of the material is influenced by deformation conditions such as temperature, strain, strain rate, microstructure of initial materials, and composition of the materials. Generally, the flow stress of the material can affect the required energy for forming and microstructure through the work hardening (WH), dynamic recovery (DRV) and dynamic recrystallization (DRX) in the hot deformation process. Several researches are conducted the experimental work on Al alloys and MMC to study the hot deformation behavior during a compression test. They have been studied the flow stress behavior and developed the constitutive models to predict the flow stress behavior for various deformation conditions [5-13]. Seetharam et al. [14-17] studied the workability, densification and hardness behavior of sintered Al–B_4C composite and developed the mathematical models to predict the grain size of the composite.

The modeling of the constitutive equation of hot deformation is necessary for estimating the failure, understanding the phenomenon, the cost of design, and the lifetime of the product. Thus, many studies have been performed on wrought metals and its alloys as well as powder metals and reported the flow behavior while hot upsetting of the same. Hence, it is essential to investigate the deformation process, flow stress behavior and development of a constitutive model with various process parameters for better performance of the metals.

Narayan and Rajeshkannan [18] performed cold upsetting tests on sintered iron–0.35% carbon to study densification behavior. They mentioned that the deformation behavior of the materials fabricated by powder metallurgy route is different from that of the cast/wrought materials (fully dense) because of the presence of more numbers of pores in the powder preforms, thereby limiting the deformation of the materials. Further, the volume of the pores is minimized during the deformation of sintered powder compacts this increasing density. Besides, Narayanasamy et al. [19] conducted cold upsetting tests on aluminium–3.5% alumina to study the effect of hardening on workability and densification. They discussed that the WH and flow stress of the materials is increased during the plastic deformation process, thus the sintered powder compacts undergo geometric hardening and densification hardening. Venugopal et al. [20] conducted ring–compression tests on sintered iron preforms for various relative densities. They found that the friction between works and tools is more in the powder performs.

The limited work related to the hot upsetting behavior of sintered material by considering the IRD and deformation conditions is found. The information regarding the hot deformation performance of sintered Al–B_4C composite is limited. Hence, the experimental works have been conducted on sintered Al–4%B_4C composite to study the flow stress behavior for various IRDes and various deformation conditions during hot upsetting. The constitutive model was developed in terms of IRD of sintered Al–4%B_4C composite to predict flow stress. The activation energy of sintered Al–4%B_4C composite was calculated for different IRDes and compared with existing literature.

2. Materials and experimental procedures

The average particle size of aluminium powder is 45 µm and purchased from SR Laboratories, Mumbai, India. Its purity is 99% and irregular in shape as shown in Figure. 1a. The ceramic reinforcement of boron carbide average size is 45 µm and procured from supertek dies, Delhi, India. It is irregular morphology in nature as shown in Figure. 1b. Al powder and 4%B_4C were carefully blended to get a homogenous mix in a pot mil about 60 min. The blended Al–4%B_4C powder was compacted with a diameter and height of 15 mm. The various IRDes of preforms is obtained by applying different compaction load and to minimize the friction between punch and die Zinc stearate is used as a lubricant. Further, the green preforms were sintered in an electric muffle furnace for a period of 1 hr. at 550 ± 10 ºC followed by cooling at room temperature. The initial diameter and height of sintered preforms and density were measured by using Vernier calipers and Archimedes's principle, respectively. The hot upset test was conducted on the hydraulic press (capacity of 50 tons) between two flat dies at various temperatures of 573 K, 673 K and 773 K and strain rates of 0.1, 0.2 and 0.3 s^{-1} and for IRDes of 80%, 85% and 90%. During the compression test, cylindrical compacts were heated for 30 min. (Soaking time) at test temperature to have a homogenous temperature. The progressive loads were applied to the cylindrical compacts until the appearance of first visible cracks on the circumference of the compacts. From the data–log unit of the hydraulic press the load-displacement data are recorded.

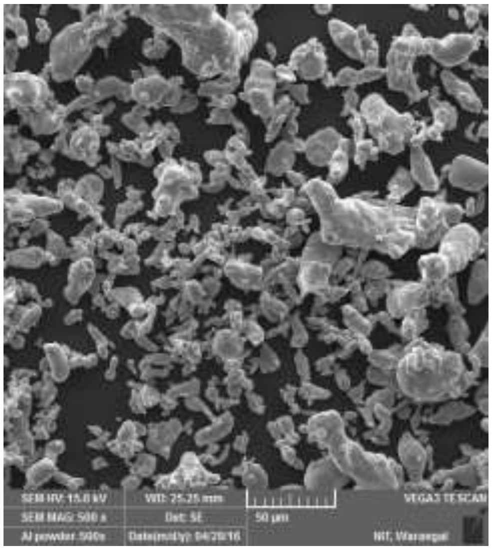

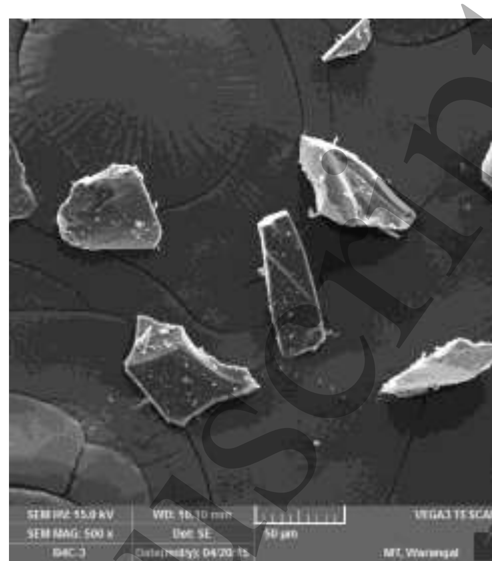

Figure. 1a SEM image of aluminium powder. Figure. 1b SEM image of boron carbide powder.

3. Results and discussion

3.1. Hot deformation curves

The true stress (σ) – true strain (ε) curves of sintered Al–4%B_4C preforms with different IRDes for various temperatures and strain rate have been demonstrated in Figures. 2– 4. It is noted that the flow stress is varied for different temperatures, strain rates, and IRDes. Figure. 2a shows the relationship between σ–ε of sintered Al–4%B_4C preforms with IRD of 80% and strain rate of 0.1 s^{-1} for various temperatures such as 573 K, 673 K, and 773 K. It is noticed that the flow stress decreased with increasing temperature because of thermal softening and highest flow stress was found at low temperature. A similar kind of behavior is noticed for other preforms irrespective of strain rates and IRD of sintered Al–4%B_4C preforms in Figures. 2–4. The flow stress difference is more between 673 K and 773 K for 80% IRD irrespective of the strain rate. During the upsetting process with lower IRD, the dislocation movement increases with increasing forming temperature and it is probably peak at 773 K. In Figure. 2, the graphs have been drawn between σ–ε with IRD of 80% for various temperatures and strain rates. It is noticed that the flow stress increased with increasing strain rate because the resistance offered by the material is increased in the preforms with increasing strain rate; hence to deform the material higher load is needed. A similar kind of behavior is noticed in the remaining IRD of 85% and 90% preforms as shown in Figures. 3 and 4 respectively. Further, it is noticed that the flow stress is increased with an increasing the IRD of the composite irrespective of the temperatures and strain rates. The reason is that the strength of the composite is increased with an increasing IRD hence more deformation load is required to deform the material thus increase the flow stress [17].

At the initial stage, the σ–ε curves increase rapidly and then exhibit peak flow stress (PFS) at certain strain values after that it is constant until the end of the strain values due to work hardening and dynamic softening [21]. Sun et al. [11] revealed that in the early part of the deformation curves, dislocations multiplied considerably and the work hardening mechanism plays an important role which leads to a rapid increase in flow stress for smaller strain values. The σ–ε curves are controlled by the work hardening before starting the DRX. After the PFS value, the σ–ε curves become constant until higher strain values thus show the dynamic softening process. DRX phenomenon is followed by the DRV, which is described that the WH rate decreased with increasing strains values. According to Taleghani et al. [6], during hot upsetting the hardening and softening mechanism are happening in the powder preforms at a higher temperature. Irrespective of the IRD the dynamic softening has more at higher temperature and lower strain rate due to the mobility of grain boundaries increases and it accelerated the growth of DRX grains at the same condition [22]. Moreover, the effect of work hardening mechanism is partially or completely neutralized at higher strain values.

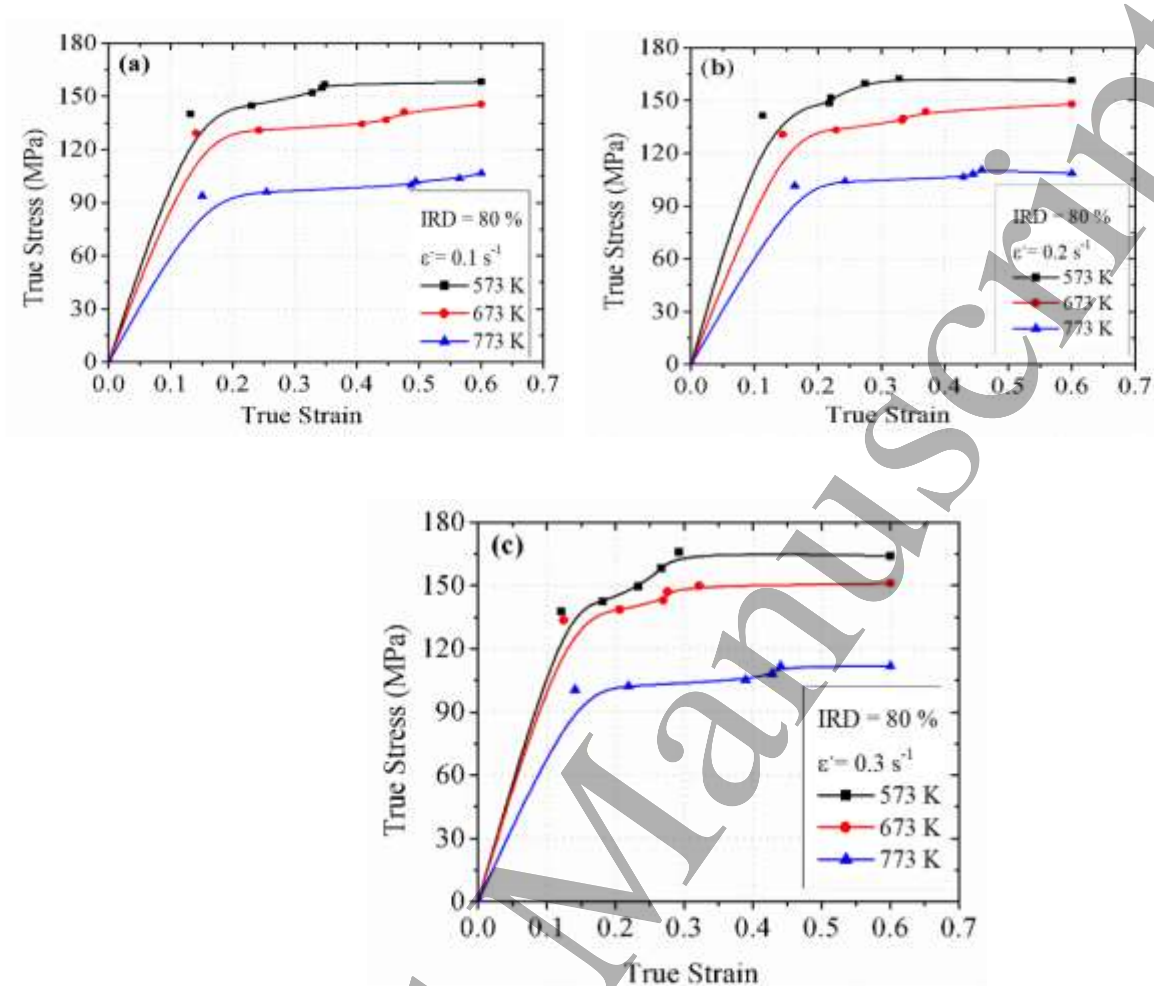

Figure. 2 True stress–true strain curves at various strain rate of Al–4%B_4C composite with of 80%.

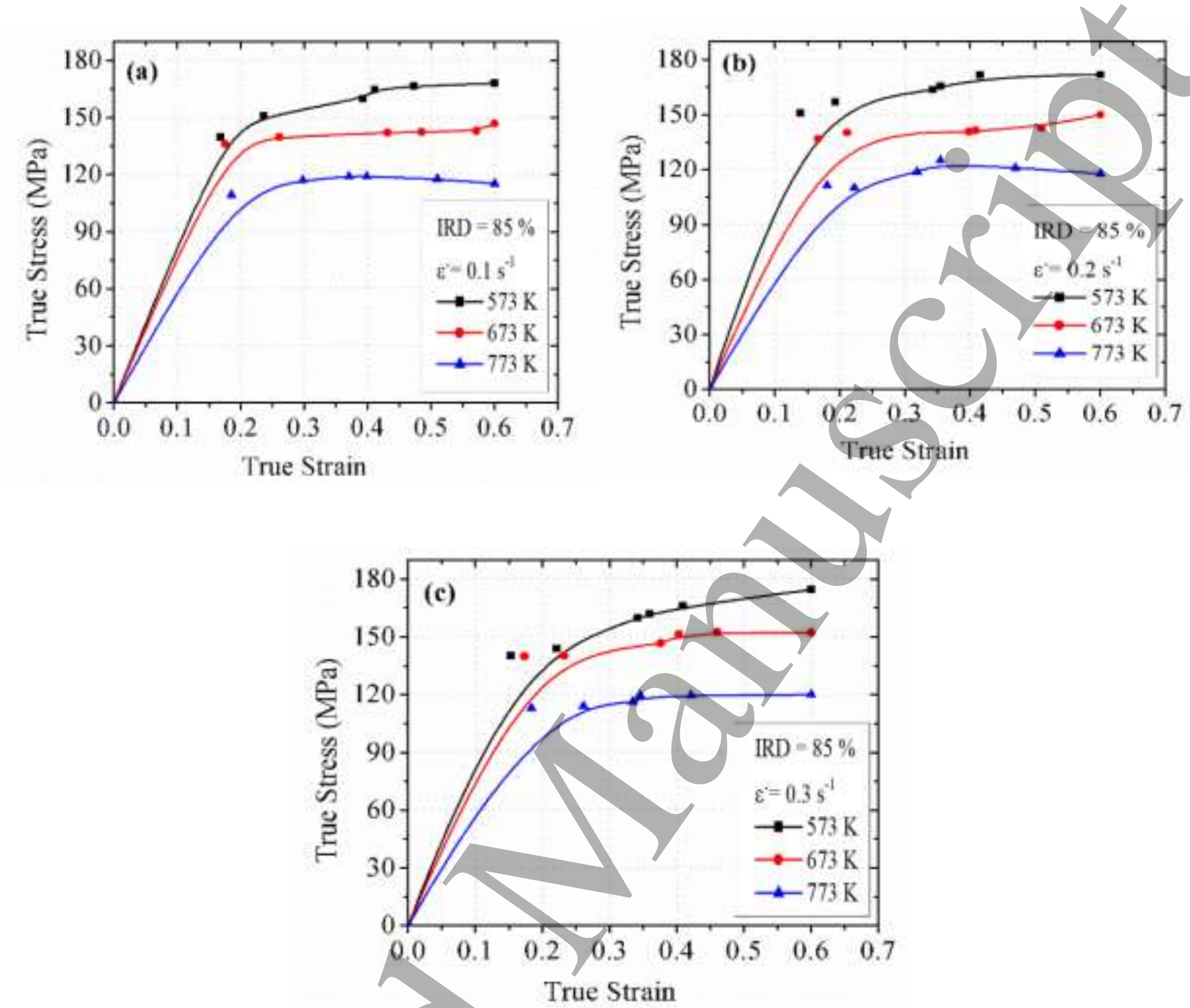

Figure. 3 True stress–true strain curves at various strain rate of Al–4% B_4C composite with of 85%.

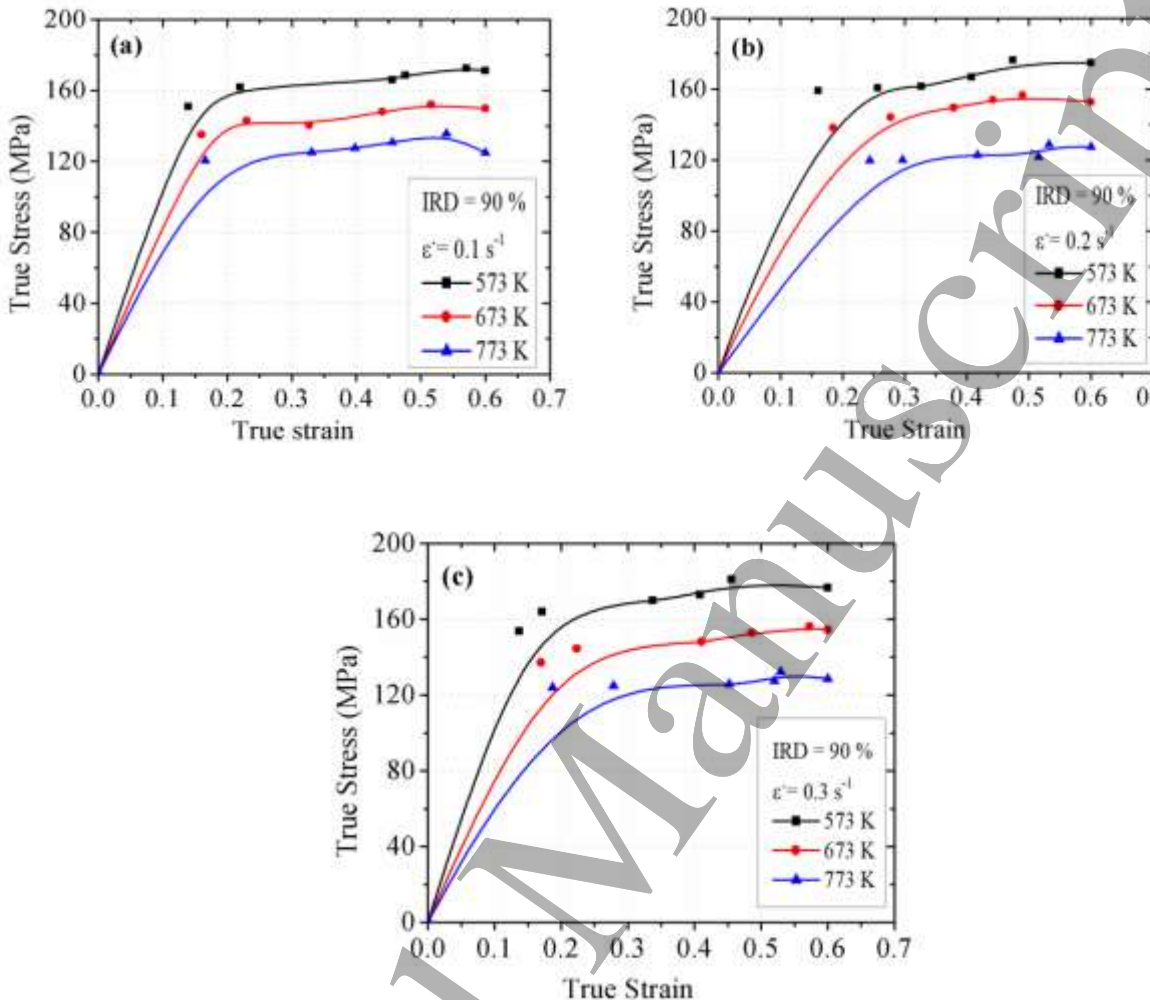

Figure. 4 True stress–true strain curves at various strain rate of Al–4%B_4C composite with of 90%.

3.2. Development of constitutive model of Al–4%B_4C composite

Generally, the Arrhenius equation is commonly adapted to describe the relationship between the flow stress and deformation condition [23, 24]. This equation could be expressed as follows:

$$\acute{\varepsilon} = A\,[\sinh\,(\alpha\sigma)]^n\, exp\left({}^{-Q}/_{RT}\right) \quad (1)$$

Where έ = strain rate (s^{-1}); σ = flow stress (MPa); n = material constant; Q = activation energy of hot deformation (KJ mol^{-1}); R = universal gas constant (8.314 J mol^{-1} K^{-1}); T = absolute temperature in Kelvin (K); A and α are material constants.

For low stress levels (ασ < 0.8), $\sinh(\alpha\sigma)^n \cong \alpha\sigma$, for high stress levels (ασ > 1.2), $\sinh(\alpha\sigma) \cong 0.5\exp(\alpha\sigma)$ and hyperbolic sine law stress function can be used for any (ασ) values. Therefore, the Arrhenius equation can be rewritten as:

$$\acute{\varepsilon} = A_1 \sigma^n \exp\left({}^{-Q}/_{RT}\right) \quad [\alpha\sigma < 0.8] \quad (2)$$

$$\acute{\varepsilon} = A_2 \exp(\beta\sigma)\ exp\ \left({}^{-Q}/_{RT}\right) \quad [\alpha\sigma > 1.2] \quad (3)$$

$$\acute{\varepsilon} = A\,[\sinh\,(\alpha\sigma)]^n \exp\left({}^{-Q}/_{RT}\right) \quad [\alpha\sigma \text{ taking any values}] \quad (4)$$

Where, $A_1 = A\alpha^n$, $A_2 = A/2^n$, and $\alpha = \beta/n$ are constants in which the β and n values are calculated from the experimental results.

Also, Zener and Hollomon [24] explained the effect of temperature and strain rate on hot deformation behavior can be evaluated through a single parameter Z, Zener–Holloman parameters (Z):

$$Z = \acute{\varepsilon} \exp\left({}^{Q}/_{RT}\right) \quad (5)$$

By substituting equation (4) into the equation (5), it gives:

$$Z = A\,[\sinh(\alpha\sigma)]^n \quad (6)$$

Furthermore, the σ can also be written in terms of Z and material constants by solving equation (6), as per the hyperbolic sine function.

$$\sigma = \frac{1}{\alpha}\ln\left\{\left(\frac{Z}{A}\right)^{\frac{1}{n}} + \left[\left(\frac{Z}{A}\right)^{\frac{2}{n}} + 1\right]^{\frac{1}{2}}\right\} \quad (7)$$

3.2.1. Calculation of material constants

As reported by Wolla et al. [10] that at higher temperatures, there is no effect of strain values on flow stress curves and it is remaining unchanged at higher values. As a result, the effect of strain on the development of above-mentioned equation (7) is not considered. Therefore, the material constants are determined at a strain value of 0.6 for sintered Al–4%B_4C composite during the hot upsetting.

The equation. (8) and (9) are obtained from the equations. (2) and (3) by applying natural logarithm, respectively.

$$\ln \acute{\varepsilon} = \ln A_1 + n \ln \sigma - \frac{Q}{RT} \quad (8)$$

$$\ln \acute{\varepsilon} = \ln A_2 + \beta\sigma - \frac{Q}{RT} \quad (9)$$

At constant temperature, the hot upsetting process was carried hence the partial differentiation of equations (8) and (9) can be simplified as:

$$n = \left[\frac{\partial ln\acute{\varepsilon}}{\partial ln\sigma}\right]_{T=const} \quad (10)$$

$$\beta = \left[\frac{\partial ln\acute{\varepsilon}}{\partial \sigma}\right]_{T=const} \quad (11)$$

The plots of lnέ–lnσ and lnέ–σ are obtained by inserting the values of flow stress and corresponding strain rate for various temperatures and IRDes into equations (10) and (11) as shown in Figure. 5 and 6, respectively. From the average slope of the lines lnέ–lnσ and lnέ–σ plots n and β values can be obtained for various temperatures, respectively. Therefore, $\alpha = \beta/n$ value is calculated. The n, β and α values are tabulated in Table 1 for sintered Al–4%B_4C composite during hot upsetting with different IRDes.

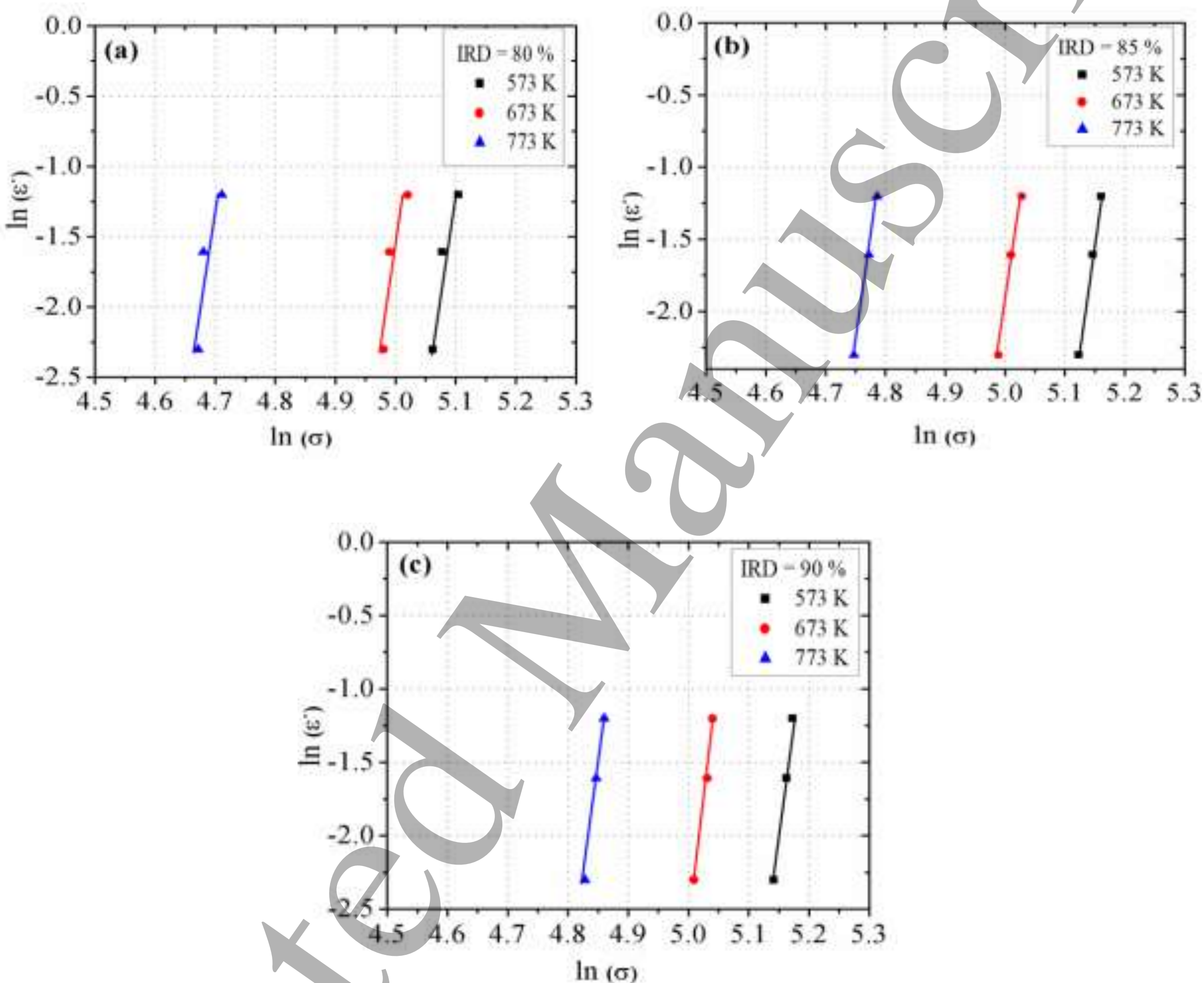

Figure. 5 Relationship between lnέ– lnσ of Al–4%B_4C composite

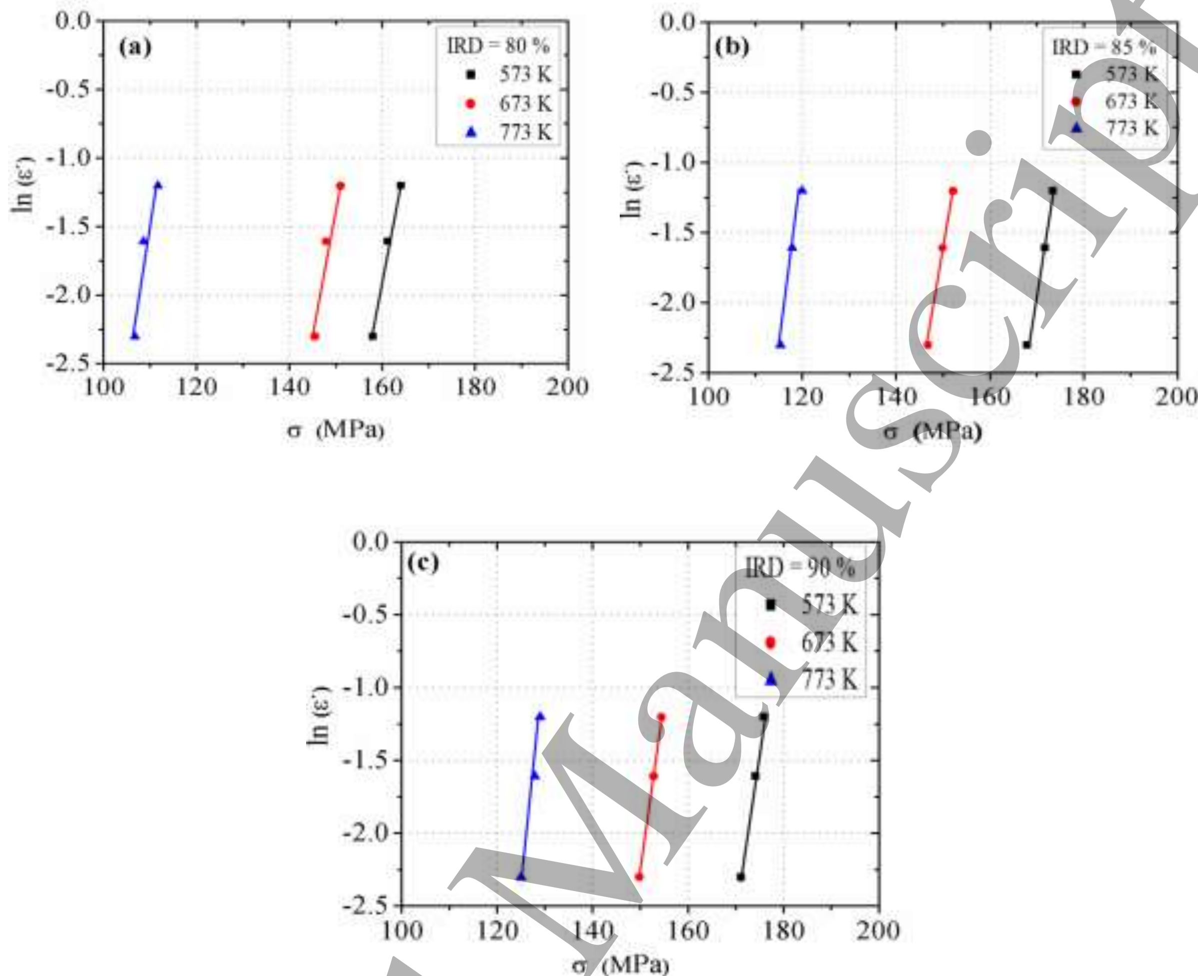

Figure. 6 Relationship between $\ln\acute{\varepsilon}$–σ of Al–4%B_4C composite

Likewise, the activation energy (Q) of sintered Al–4%B_4C composite during hot upsetting with different IRDes can be obtained by applying the natural logarithm on both sides of equation (4):

$$\ln \acute{\varepsilon} = \ln A + n \ln[\sinh(\alpha\sigma)] - \frac{Q}{RT} \tag{12}$$

For the given constant strain rate condition, partial differentiation of equation (12) gives that:

$$Q = R\left\{\frac{\partial \ln \acute{\varepsilon}}{\partial \ln[\sinh(\alpha\sigma)]}\right\}_{T=const}\left\{\frac{\partial \ln[\sinh(\alpha\sigma)]}{\partial\left(\frac{1}{T}\right)}\right\}_{\acute{\varepsilon}=const} \tag{13}$$

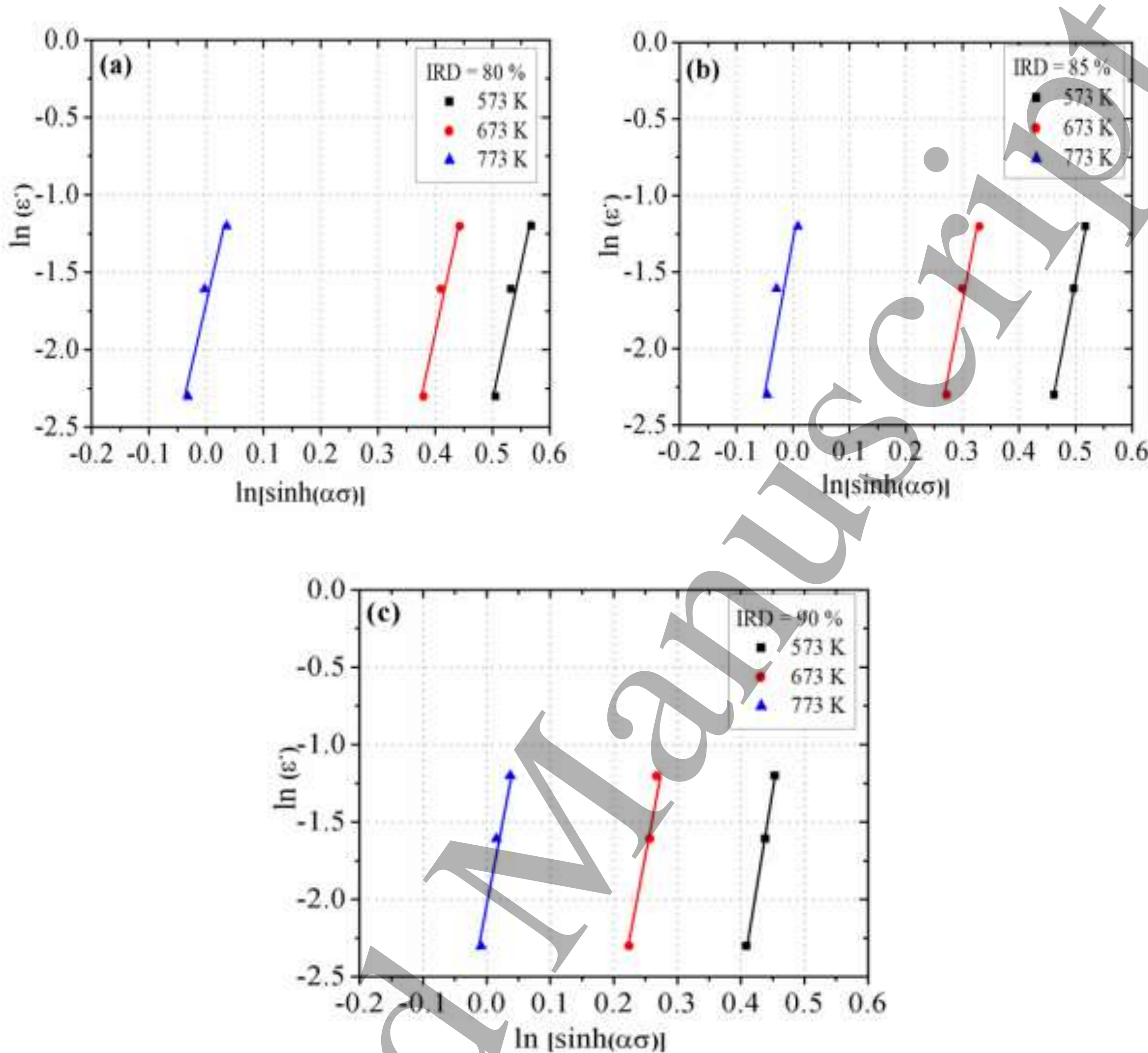

Figure. 7 Relationship between lnέ–ln[sinh(ασ)] of Al–4%B_4C composite

The relationship of lnέ–ln[sinh(ασ)] and ln[sinh(ασ)]–1/T were obtained by inserting the values of σ, α and temperature and corresponding strain rate for different IRDes into equation (13), respectively. The Q values mentioned in Table 1 for different IRDes is obtained from the relation of lnέ–ln[sinh(ασ)] and ln[sinh(ασ)]–1/T plots and are demonstrated in Figures. 7 and 8, respectively. It is noticed that the value of n, β, and Q are greatly affected by the IRD. It is also noticed that the Q values for hot deformation decrease with decreasing IRD because of the presence of more pores in the preforms, which leads to a reduction in the resistance of the material to deform. Also, the increase in IRD the Q values for hot deformation exhibited higher values. The activation energy is one of the key parameters which measures the degree of difficulty of the hot deformation of the materials. As a result, plastic deformations become more difficult with increasing IRD. The values of α were decreased with an increase in the IRD.

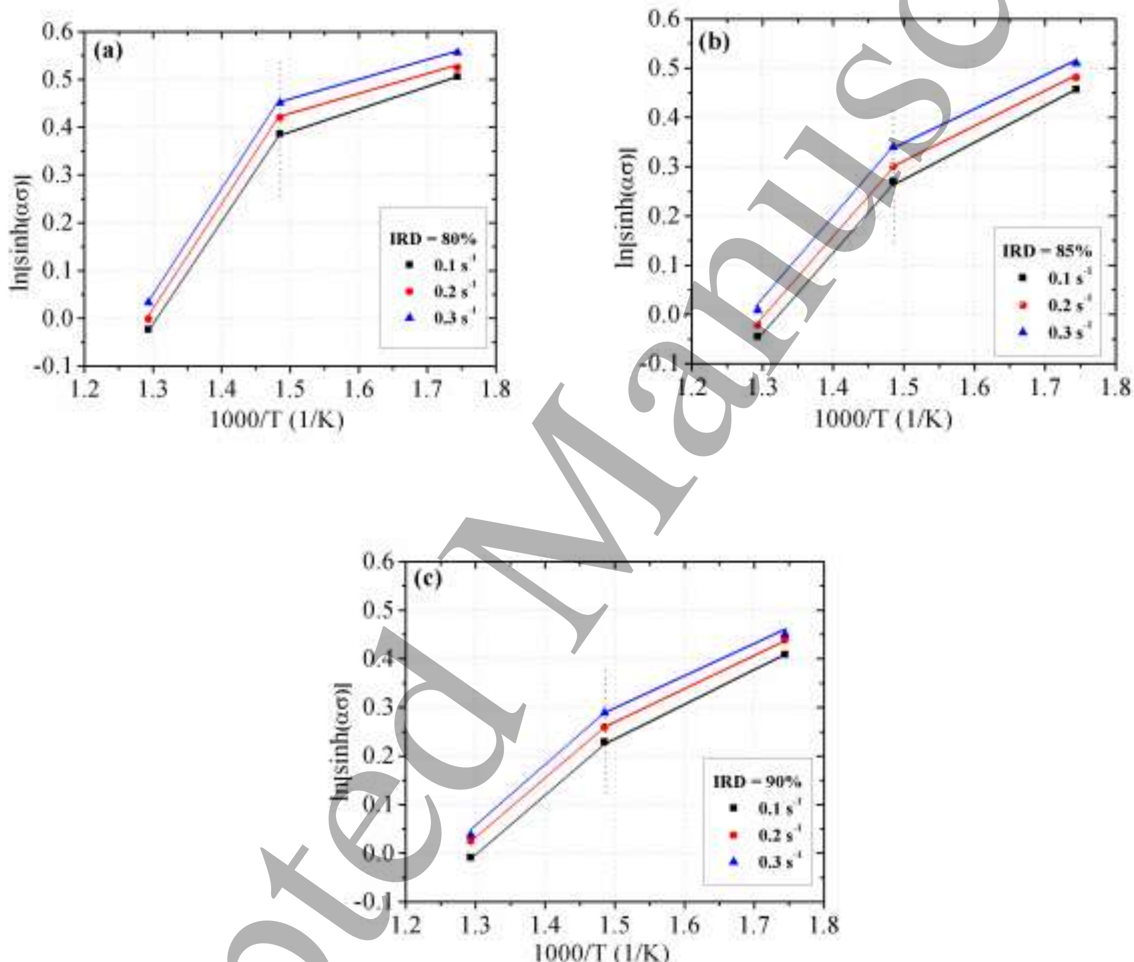

Figure. 8 Relationship between ln [sinh (ασ)]–1/T of Al–4%B_4C composite

By applying the natural logarithm of equation (6), it gives:

$$\ln Z = \ln A + n \ln[\sinh(\alpha\sigma)] \quad (14)$$

By inserting the values of Q into equation (5), Z parameter can be evaluated. The values of lnA determined from the intercept of lines lnZ–ln[sinh(ασ)] plots for different IRDes are demonstrated in Figure. 9. The values of lnA for sintered Al–4%B_4C composite with different IRDes of 80%, 85% and 90% can be found to be 21.27, 24.16 and 25.55, respectively.

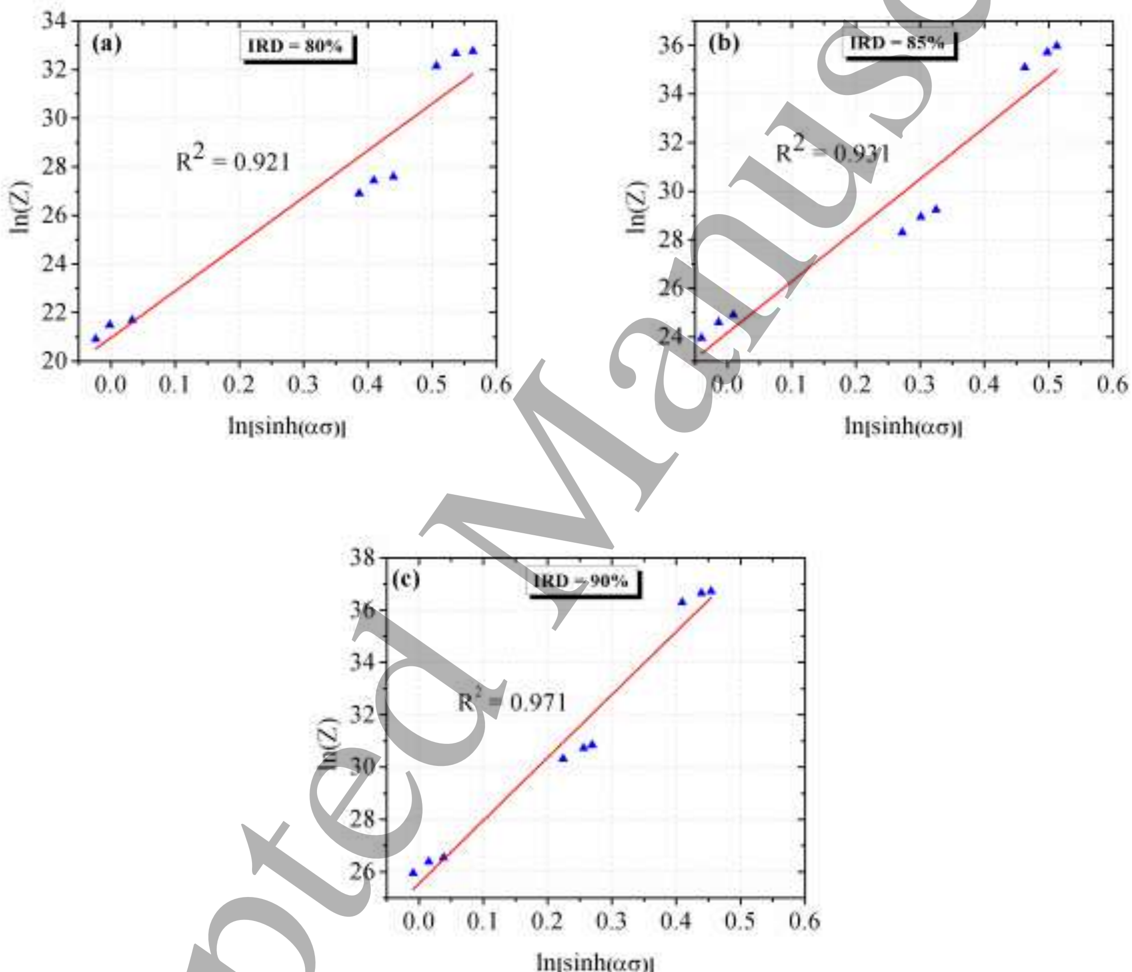

Figure. 9 Correlation between lnZ–ln[sinh(ασ)] of Al–4%B_4C composite

Figure. 9 shows that the slope values of lnZ–ln[sinh(ασ)] plots are decreasing with a decrease in IRDes. When the slope of the plot lnZ–ln[sinh(ασ)] is low, the deformation conditions slightly affected PFS of the preforms, but it is significant for higher slope irrespective of the IRDes.

The relationship between n, α, lnA and Q and IRD of sintered Al–4%B_4C composite were established by fitting data point into a polynomial function as shown in Figure. 10. Thus, the developed mathematical expression between IRD and flow stress, deformation temperature, strain rate of sintered Al–4%B_4C composite during hot upsetting tests can be expressed as follows (R^2 = correlation coefficient):

$$n = 0.0422\ IRD^2 - 6.121\ IRD + 243.8 \tag{15}$$

$$\alpha = 6E-06\ IRD^2 - 0.00113\ IRD + 0.0601 \tag{16}$$

$$Q = -0.049\ IRD^2 + 10.329\ IRD - 351.66 \tag{17}$$

$$\ln A = -0.03\ IRD^2 + 5.528\ IRD - 228.97 \tag{18}$$

Table 1. Values of β, n, α and Q with different IRDes of Al–4%B_4C composite

IRD (%)	**β**	**n**	**α**	**Q (KJ/mol)**
80	0.197	24.23	0.0081	161.06
85	0.212	28.44	0.0074	172.28
90	0.243	34.76	0.007	181.05

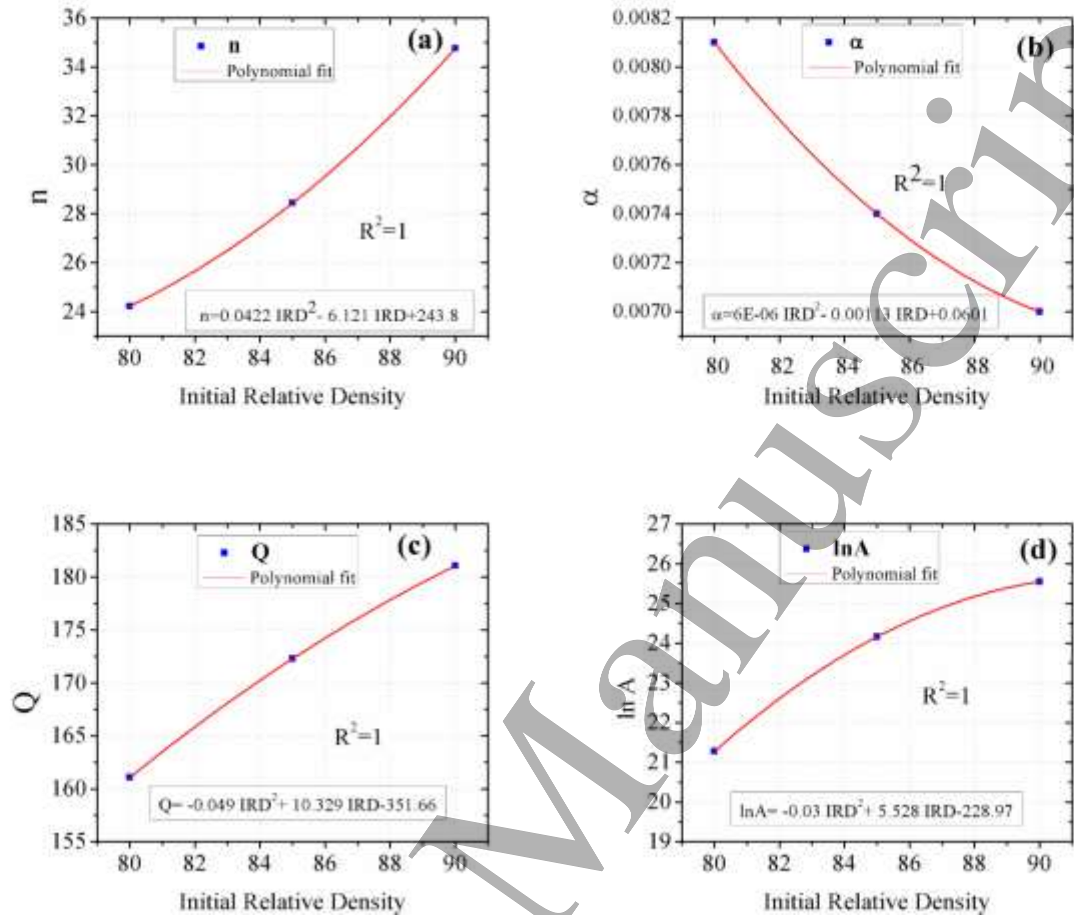

Figure. 10 Variations in (a) n (b) alpha (α) (c) Q (d) lnA with initial relative density in sintered Al–4%B_4C composite during hot upsetting test.

3.3. Validation of developed constitute equations of Al–4%B_4C composite

The predicted flow stress values determined according to equations. (7) and (15) – (18) is tabulated in Table 2. The values of predicted flow stress (σ_P) are compared with experimental flow stress (σ_E) values by plotting the graphs to assess the accuracy of the developed constitutive equation of sintered Al–4%B_4C composite for different IRDes, and shown in Figure. 11. All the experimental and predicted data are close to the best fit line which indicates the accuracy of the constitutive equation. The R^2 values are found to be 0.923, 0.977 and 0.994 for IRDes of 80%, 85%, and 90%, respectively.

Moreover, the established constitutive models for sintered Al–4%B_4C composite accuracy was confirmed by absolute error (δ) and mean absolute error (δ_m). The absolute error is calculated from predicted and experimental values by using the equation (19).

$$\delta = \left|\frac{\sigma_P - \sigma_E}{\sigma_E}\right| X\ 100\ \% \quad (19)$$

The detailed comparisons were made between the predicted and experimental results of sintered Al–4%B_4C composite for various temperatures and strain rates with different IRDes are shown in Table 2. The absolute error does not exceed 10.6% and means absolute error does not exceed 9.95% for various IRDes and deformation conditions. The maximum mean absolute error is not exceeding 9.95% and it is acceptable considering the complexity of the deformation behavior of porous materials.

The established constitutive model has a good predictive capability for Al–4%B_4C composite during hot upsetting for all investigated temperatures and IRDes. Accordingly, the predicted results are well satisfied with the experimental result, which verifies the accuracy of the developed constitutive model for sintered Al–4%B_4C composite during the hot upsetting test.

Table 2. Comparison between experimental and predicted peak flow stress of sintered Al–4%B_4C composite

Def. Tem. (K)	**$\acute{\varepsilon}$ (s^{-1})**	**IRD = 80%**				**IRD = 85%**				**IRD = 90%**			
		σ_E MPa	σ_P MPa	δ (%)	δ_m (%)	σ_E MPa	σ_P MPa	δ (%)	δ_m (%)	σ_E MPa	σ_P MPa	δ (%)	δ_m (%)
573	0.1	158.02	169.41	7.21		167.97	172.26	2.55		171.13	174.00	1.68	
573	0.2	160.90	171.64	6.71	6.4	171.98	174.89	1.69	1.67	173.16	175.28	1.22	1.02
573	0.3	164.32	173.11	5.35		174.68	176.02	0.77		175.24	175.22	0.16	
673	0.1	145.54	134.26	7.75		146.81	136.49	7.03		150.26	144.37	3.92	
673	0.2	147.67	136.42	7.67	8.1	149.93	138.86	7.39	7.54	151.61	145.68	3.91	4.27
673	0.3	151.15	137.68	8.91		152.68	139.95	8.22		153.76	146.00	5.01	
773	0.1	106.78	98.38	7.87		115.28	104.37	9.46		124.87	115.48	7.52	
773	0.2	108.65	100.19	7.78	8.31	117.21	106.31	9.30	9.95	127.10	116.68	8.20	8.02
773	0.3	111.71	101.34	9.28		119.97	107.24	10.6		127.81	117.11	8.37	

Further, the ability of the developed constitutive equation for predicting the peak flow stress of sintered Al–4%B_4C composite was evaluated by calculating the peak flow stress with IRD of 88%. The predicted flow stress of sintered Al–4%B_4C composite of 88% initial relative density for various temperatures and strain rates is compared with experimental peak flow stress of the same condition and as shown in Table 3. The experimental peak flow stress values of the sintered Al–4%B_4C composite of 88% IRD were not used to develop the constitutive equation. It is noticed from Table 3 that the average mean absolute error is 5.97, which indicates the developed constitutive model was capable to predict accurately the peak flow stress of the performs.

Table 3. Comparison between experimental and predicted peak flow stress of sintered Al–4%B_4C composite of initial relative density 88%

Def. Tem. (K)	$\acute{\varepsilon}$ (s^{-1})	IRD = 88%			
		σ_E MPa	σ_P MPa	δ (%)	δ_m (%)
573	0.1	169.25	156.61	7.46	7.97
573	0.2	173.17	159.07	8.13	
573	0.3	175.15	160.52	8.34	
673	0.1	148.41	137.59	7.28	7.49
673	0.2	151.17	139.90	7.45	
673	0.3	153.12	141.25	7.74	
773	0.1	122.08	124.37	1.88	2.47
773	0.2	123.26	126.55	2.67	
773	0.3	124.25	127.83	2.88	
Average					5.97

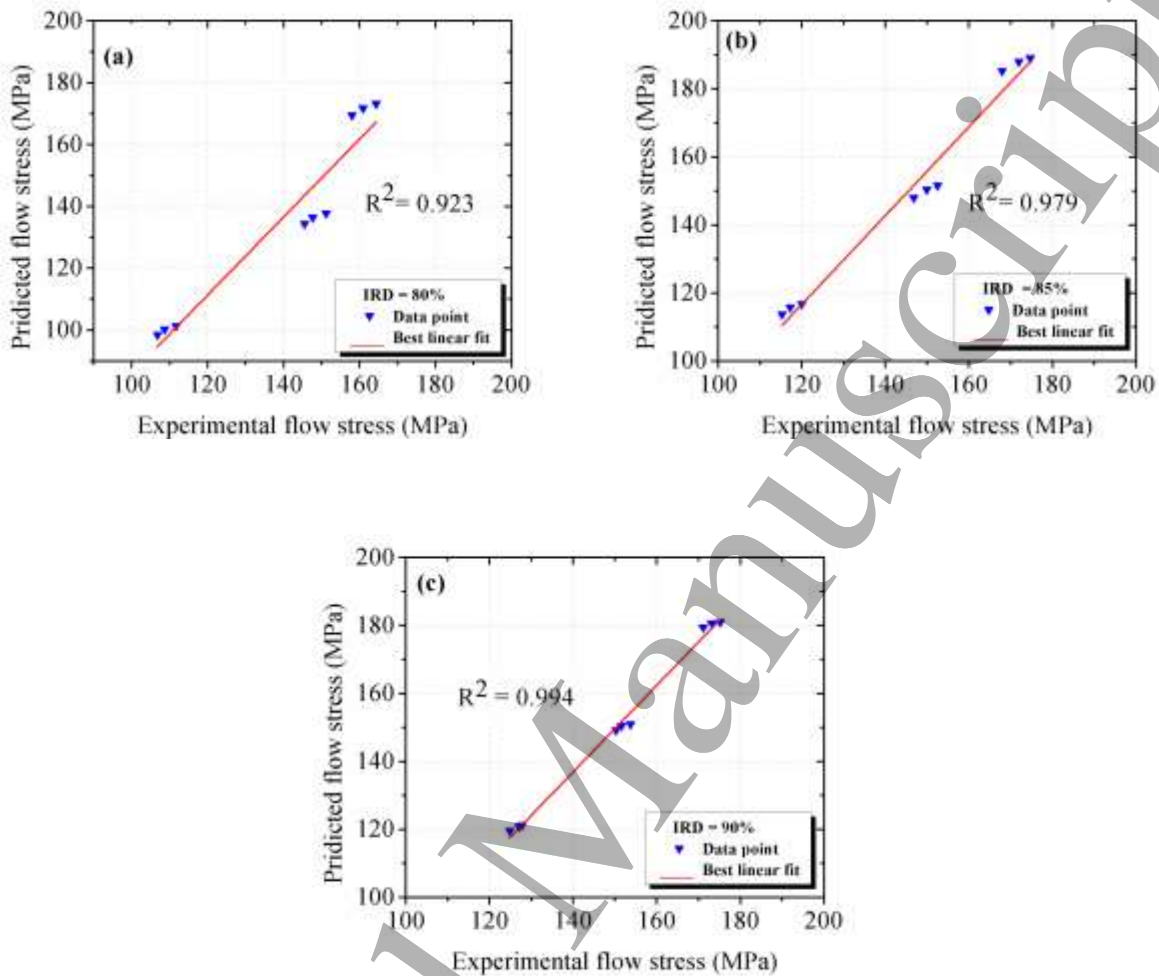

Figure. 11 Correlation between experimental and predicted results of sintered Al–4%B_4C composite

4. Activation energy of sintered Al–4%B_4C composite

The average activation energy (Q) of sintered Al–4%B_4C composite was calculated for various IRDes during the hot upsetting test, which is higher than the value of pure aluminum as shown in Table 4. It was reported [25, 26] that the activation energy of aluminum metal matrix composite for hot deformation was higher than that of aluminum. The dislocation motion is impeded by the existing B_4C particles in the composite. It was concluded that the obtained activation energy of sintered Al–4%B_4C preforms for different IRDes is acceptable. The occurrence of higher activation energy during the upsetting tests of composite materials is due to the transformation of the deformation load to reinforcement by the matrix [25, 26], whereby an interfacial diffusion is considerably slower, which increases the activation energy of composite materials.

Table 4. Activation energies (Q) (KJ/mol) for different compositions

Composition	Fabrication Route	Activation energy (Q) (KJ/mol)			Reference
		IRD			
Al–4%B_4C	Powder metallurgy	80%	85%	90%	Present investigation
		161.08	172.28	181.05	
Pure aluminum	Casting	144.3			[27]

5. Conclusions

The hot deformation behavior of sintered Al–4%B_4C composite with various IRDes of 80%, 85%, and 90% was studied by performing the hot upsetting test for various temperatures of 573 K, 673 K and 773 K and strain rates of 0.1 s^{-1}, 0.2 s^{-1} and 0.3 s^{-1}. The following conclusion can be drawn:

1. The influences of the IRD and deformation conditions on the σ–ε curves are significant for all tested conditions. The flow stress curves increase with increasing IRD and strain rate, whereas decreases with deformation temperature.

2. The IRD has a great influence on the hot deformation behavior of sintered Al–4%B_4C composite. The activation energy of hot deformation was exhibited at higher values due to an increase in IRD.
3. The constitutive equations were developed between material constants and IRD for predicting the flow stress of sintered Al–4%B_4C composite precisely.
4. The comparison was made between the predicted and experimental values and it shows good agreement. The absolute errors were not exceeding 10.6% and mean absolute error does not exceed 9.95% for various IRDes and deformation conditions.
5. The activation energy (Q) calculated for sintered Al–4%B_4C composite with IRDes of 80%, 85%, and 90% was 161.06, 172.28 and 181.05 KJ/mol, respectively. This range of values is higher than the value of pure aluminum (144.3 KJ/mol).

Acknowledgement

R. Seetharam thanks to National Institute of Technology Warangal (NITW) research fellowship issuing by Ministry of Human Resource Development (MHRD), India.

References

[1] Cambronero L E G, Sanchez E, Ruiz-Roman J M and Ruiz-Prieto J M 2003 Mechanical characterisation of AA7015 aluminium alloy reinforced with ceramics J. Mater. Process. Technol. **143** 378–383.

[2] Nair S V, Tien J K and Bates R C 1985 SiC–reinforced aluminum metal matrix composites Int. Met. Rev. **30** 275–290.

[3] Abenojar J, Velasco F and Martinez M A 2007 Optimization of processing parameters for the Al+10% B_4C system obtained by mechanical alloying J. Mater. Process. Technol. **184** 444–446.

[4] William C and Jr. Harrigan 1998 Commercial processing of metal matrix composites, Mater. Sci. Eng. A **244** 75–79.

[5] Jin W, Jun C, Zhen Z and R. Xue-yu 2007 Hot deformation behavior and flow stress model of F40MnV steel J. Cent. South. Univ. Technol. **141** 19−23.

[6] Taleghani M A J, Navas E R, Salehi M and Torralba J M 2012 Hot deformation behaviour and flow stress prediction of 7075 aluminium alloy powder compacts during compression at elevated temperatures Mater. Sci. Eng. A **534** 624–631.

[7] Guo J, Zhao S, Murakami R, Ding R and Fan S 2013 Modeling the hot deformation behavior of Al alloy 3003 J. Alloys Compd. **566** 62–67.

[8] Gangolu S, Rao A G, Prabhu N, Deshmukh V P and Kashyap B P 2014 Hot workability and flow characteristics of aluminum–5wt.% B_4C composite J. Mater. Eng. Perform. **23** 1366–1373.

[9] Zhang R Y, Shi Z M and Zhang X M 2015 Hot deformation behavior and microstructure evolution of TiC–Al_2O_3/Al composites Rare Met. **34** 725–730.

[10] Wolla W D, Davidson M.J and Khanra A K 2015 Constitutive modeling of powder metallurgy processed Al–4%Cu preforms during compression at elevated temperature Mater. Des. **65** 83–93.

[11] Sun Y, Ye W H and Hu L X 2016 Constitutive modeling of high–temperature flow behavior of Al–0.62Mg 0.73 Si aluminum alloy J. Mater. Eng. Perform. **25** 1621–1630.

[12] Mirzadeh H 2014 Constitutive analysis of Mg–Al–Zn magnesium alloys during hot deformation Mech. Mater. **277** 80–85.

[13] Mirzadeh H 2015 Constitutive behaviors of magnesium and Mg-Zn-Zr alloy during hot deformation Mater. Chem. Phys. **152** 123-126.

[14] Seetharam R, Subbu S K and Davidson M J 2017 Hot workability and densification behavior of sintered powder metallurgy Al-B_4C preforms during upsetting J. Manuf. Processes. **28** 309-318.

[15] Seetharam R, Subbu S K and Davidson M J 2017 Influence of temperature on the workability and hardness of sintered Al-4wt.%B_4C in upsetting Procedia. Eng. **173** 910-917.

[16] Seetharam R, Subbu S K and Davidson M J 2018 Analysis of grain size evolution of sintered Al-4wt.%B_4C preforms subjected to hot compression test Metall. Microstruct. Anal. **7(2)** 176-183

[17] Seetharam R, Subbu S K and Davidson M J 2018 Microstructure modeling of dynamically recrystallization grain size of Al-4wt.%B_4C composite during hot upsetting J. Eng. Mater. Techno. **1401(2)** 021003.

[18] Narayan S and Rajeshkannan S 2011 Densification behaviour in forming of sintered iron–0.35% carbon powder metallurgy preform during cold upsetting, Mater. Des. **32** 1006–1013.

[19] Narayanasamy R, Anandakrishnan V and Pandey K S 2008 Effect of geometric work–hardening and matrix work-hardening on workability and densification of aluminium–3.5% alumina composite during cold upsetting Mater. Des. **29** 1582–1599.

[20] Venugopal P, Venkatraman S, Vasudeva R and Padmanabhan K A 1988 Ring – compression tests on sintered iron performs J. Mech. Work. Technol. **16** 51–64.

[21] Lin Y C, Shun-Cun L, Liang-Xing Y and Huang J 2018 Microstructural evolution and high temperature flow behaviors of a homogenized Sr- modified Al-Si-Mg alloy J. Alloys and Compd. **739** 590-599.

[22] Mandal S, Rakesh V, Sivaprasad P V, Venugopal S and Kasiviswanathan K V 2009 Constitutive equations to predict high temperature flow stress in a Ti-modified austenitic stainless-steel Mater. Sci. Eng., A **500** 114–121.

[23] Lin Y C and Xiao-Min C 2011 A critical review of experimental results and constitutive descriptions for metalsand alloys in hot working Mater. Des. **32** 1733–1759.

[24] Zener C and Hollomon J H 1944 Effect of strain rate upon plastic flow of steel J. Appl. Phys. **15** 22–32.

[25] Mishra R S, Bieler T R and Mukherjee A K 1995 Superplastisity in powder metallurgy aluminum alloys and composites Acta. Metall. Mater. **43** 877–891.

[26] Li Y and Langdon T G 1998 High strain rate superplastisity in metal matrix composites: The role of load transfer Acta Mater. **46** 3937–3948.

[27] Gale W F and Totemeier T C 2003 Smithells Metals Reference Book, seventh ed., Butterworth-Heinemann, Burlington, VT.